

the other data presented in Table VII. Here the experimental molar conductivity at 430 and 475 °C, Λ_{exptl} , is obtained from eq 7 by using the measured densities and conductivities. The calculated molar conductivity Λ_{calcd} is obtained from eq 8 by using values of $\Lambda_{\text{K}_2\text{S}_2\text{O}_7}$ and $\Lambda_{\text{V}_2\text{O}_5}$ calculated on the basis of the general polynomial for the density (Table III) and the specific conductivities of molten $\text{K}_2\text{S}_2\text{O}_7$ and V_2O_5 (in the extrapolated liquid state¹⁹). The percentage difference between Λ_{exptl} and Λ_{calcd} is also calculated. The very large negative deviation (up to around -60%) suggests²⁰ that most probably complexes are formed in the system. Usually²⁰ complex formation is considered to take place for deviations higher than about 5%. The restricted ability for the melt to dissolve more V_2O_5 when $X_{\text{V}_2\text{O}_5}$ is 0.5 indicates that V_2O_5 is probably only soluble in the melt when residual pyrosulfate ions are present. This investigation also indicates that monomeric complexes, VO_2SO_4^- and $\text{VO}_2\text{SO}_4\text{S}_2\text{O}_7^{4-}$, might only be important in melts very dilute with respect to V_2O_5 and that they might not be formed to any appreciable extent at higher mole fractions of V_2O_5 (since no signs of breaks are found on the density or con-

ductivity curves at $X_{\text{V}_2\text{O}_5} = 0.25$).

The possible structures of the complexes $(\text{VO}_2)_2(\text{SO}_4)_2\text{S}_2\text{O}_7^{4-}$ and $(\text{VO}_2\text{SO}_4)_n^{n-}$ have been discussed recently.¹⁴ The former probably contains an oxygen double bridge and bidentate coordinate sulfate and pyrosulfate ions making the coordination number of 6 possible for vanadium. The latter is probably a chain like complex where the vanadium atoms with a coordination number of 4 are linked together with bidentate coordinate sulfate ions. Further evidence for the existence and structures of the species proposed in this paper is being sought through planned NMR, IR, and X-rays investigations on liquids and solids of the V_2O_5 - $\text{K}_2\text{S}_2\text{O}_7$ system.

Acknowledgment. This investigation has been supported by the Danish Technical Science Research Foundation, the French National Center of Scientific Research, and the European Economic Communities (EEC) in accordance with contract No. STI-011-J-C(CD).

Registry No. V_2O_5 , 1314-62-1; $\text{K}_2\text{S}_2\text{O}_7$, 7790-62-7.

Concentration-Dependent Main-Chain Dynamics of Sodium Polyacrylate As Probed by NMR in the Semidilute Regime

C. J. M. van Rijn, W. Jesse, J. de Bleijser, and J. C. Leyte*

Gorlaeus Laboratories, Department of Physical and Macromolecular Chemistry, University of Leiden, Leiden, The Netherlands (Received: April 15, 1986; In Final Form: August 26, 1986)

Sodium polyacrylate chains exhibit reduced reorientational mobility in the semidilute regime as probed by frequency-dependent nuclear magnetic relaxation experiments. Nuclear magnetic relaxation rates of deuterons have been measured in aqueous solutions of methylene-deuteriated poly(acrylic acid) (CD_2 -PAA). Upon diluting a neutralized solution of CD_2 -PAA (sodium polyacrylate), a sharp increase of the transverse relaxation rate R_2 was observed, whereas the longitudinal relaxation rate R_1 remained unaffected. It is shown that in the semidilute regime slow motions with correlation times $> 10^{-8}$ s show up irrespective of the fast (internal) motions with correlations times $\sim 10^{-9}$ s. The origin of these slow motions is indicated by polyelectrolyte theory; the large correlation times are probably due to the enhanced (electrostatic) stiffness of the CD_2 -PAA chain in the semidilute regime. In concordance with this idea is the fact that the large correlation times decrease when a simple salt (NaCl) is added to the solution. An implication for the interpretation of counterion relaxation is discussed.

Introduction

This paper reports a NMR study on dynamic chain behavior of methylene-deuteriated poly(acrylic acid) (CD_2 -PAA). Whereas proton relaxation is usually dependent on intra- and intermolecular motion, deuteron relaxation is completely determined by the reorientational motion of the CD bonds in the polyacrylic acid chain. Deuteron relaxation is therefore a particularly suitable source of information on chain dynamics.

An interesting topic in polyelectrolyte physics is the relaxation between the stiffness of a polyelectrolyte chain and its dynamic behavior^{1,2} as probed by NMR relaxation. As will be discussed in more detail in other sections, this relation is by no means simple and straightforward. From a sufficiently extended NMR investigation one may obtain values of the spectral density function $J(\omega)$ for the time-dependent process driving the relaxation, at a certain number of frequencies. This set of numerical values may be transformed to a set of correlation times if the functional shape of $J(\omega)$ is known or assumed. For rotation diffusion models the correlation function reduces to a sum of exponentials and $J(\omega)$ is then represented by a sum of Lorentzians. Under the assumption of rotation diffusion, relaxation rates of a polymer nucleus such

as ^2H usually yield more than one correlation time, a typical result being three correlation times.

In the next stage of interpretation these correlation times should be related to some representation of (part of) the polymer molecule. For sufficiently long polymer molecules the order of magnitude of the correlation times usually indicates that overall motion of the complete molecule cannot be the motional process involved: the dynamical unit is often considerably smaller than the polymer. Thus one is led to the concept of a dynamical persistence length, i.e., the length of polymer chain involved in correlated motion. For flexible polymers in solution it may be expected that this dynamic persistence length corresponds roughly with the conformational persistence length. On relating the correlation times to a prolate Perrin ellipsoid, its short and long semiaxes will be tentatively identified with the thickness and persistence length of poly(acrylic acid). If as another example the model of a spherical reorienting dynamical unit (with one internal rotation mode) is used, the radius of the sphere will, again tentatively, be identified with the persistence length of the polymer. Comparison with experimental estimates of these lengths should then lead to conclusions on the appropriateness of the motional model.

Poly(acrylic acid) in aqueous solution may be considered an interesting polyelectrolyte model system by virtue of the small intrinsic persistence length³ (~ 10 Å) of the main chain and the

(1) Yamakawa, H. *Modern Theory of Polymer Solutions*; Harper & Row: New York, 1971.

(2) Yamakawa, H.; Fujii, M. *J. Chem. Phys.* **1984**, *81*, 997.

TABLE I: Relaxation Rates R_1 and R_2 (in s^{-1}) of CD_2 -PAA (DP = 850) at Three Larmor Frequencies^a

no.	C_p , monomol/L	α	$\omega_0 = 4.6$ MHz				$\omega_0 = 9.2$ MHz				$\omega_0 = 41.4$ MHz			
			R_1	R_2	R_{2s}	R_{2f}	R_1	R_2	R_{2s}	R_{2f}	R_1	R_2	R_{2s}	R_{2f}
S ₉	0.25	0.1	356	367			321	351			201	269		
S ₁₀	0.07	0.1	322	337			281	318			191	249		
S ₁	0.23	0.78	415	476	434	524	373	459	408	507	211	352	320	390
S ₂	0.082	0.78	416	615	435	865	316	545	410	795	218	450	315	710
S ₃	0.026	0.78	421	745	435	1655	333	696	401	1606	209	590	290	1500
S ₄	0.012	0.78	422	950	520	2000	300	860	475	2110	191	750	365	2020

^a Estimated errors are 5% for R_1 and R_2 . Nonexponential decays were resolved in two exponents R_{2s} and R_{2f} . The error bars in R_{2s} are the same as for R_2 and nearly doubled for R_{2f} .

variability of its electrostatic persistence length.

At low ionic strength the total persistence will be mainly determined by the electrostatic persistence contribution due to the repulsive charges along the polyelectrolyte chain.⁴⁻⁷ On decreasing the ionic strength of the solution, the persistence length of CD_2 -PAA will increase and this will result in a decrease of the reorientational mobility of the chain.

In view of the emergence of some polymer theoretical concepts in the previous remarks the meaning of these concepts in polyelectrolyte theory will be briefly presented here.

The study of polyelectrolyte solutions is concerned with the structural and dynamic behavior of polyions and its dissociated counterions in a solvent. The interrelation between the long polyions, the small counterions and the solvent is mainly determined by the long-range Coulomb interaction. Roughly speaking, one can say that the equally charged polyions seem to avoid each other, while the counterions with opposite charge tend to cluster around the polyions, thereby screening the electrostatic fields of the polyions.

It was the cell model⁴ in which these features, together with the assumption of axial symmetry around the polyion, were incorporated. In the salt-free case an analytic solution has been obtained for the electrostatic field around the polyion by using the well-known Poisson-Boltzmann equation. The range of the electrostatic field depends strongly on the ionic strength and the degree of neutralization (relative fraction of charged groups). In concentrated solutions these fields may persist several angstroms, whereas in dilute solutions the range can yield values of several hundred angstroms.

The electrostatic field around the polyion will also change the structure of the polyion itself. Especially at low ionic strength the backbone of the polyion will stiffen as result of the repulsion between the equal charges along the polyion chain.

When the total stiffness of the polyion chain is determined by local interactions a statistical expression for chain stiffness¹ is valid

$$\langle \hat{\mu}(t) \cdot \hat{\mu}(s) \rangle = \exp[-|t - s|/L_t] \quad (1)$$

where $\hat{\mu}(t)$ is the direction of the chain at contour point A , s, t are contour parameters along the chain, and L_t is the static persistence length.

The static persistence length L_t describes the decrease of the orientation correlation along the contour. In polyelectrolyte theory^{5,6} the static persistence length L_t can be considered as the sum of two contributions: the bare or intrinsic persistence length L_p , and the electrostatic persistence length L_e . The former is a steric property of the uncharged polyelectrolyte and the latter is the contribution to chain direction correlation by all electrostatic interactions.

In the approximation of local stiffness⁷ ($L_t > \kappa^{-1}$), the following expression for the electrostatic persistence length has been obtained

$$L_e = f^2 Q / 4\kappa^2 A^2$$

$$\text{with } f = 1 \text{ for } \lambda \equiv Q/A < 1, \quad f = A/Q \text{ for } \lambda > 1 \quad (2)$$

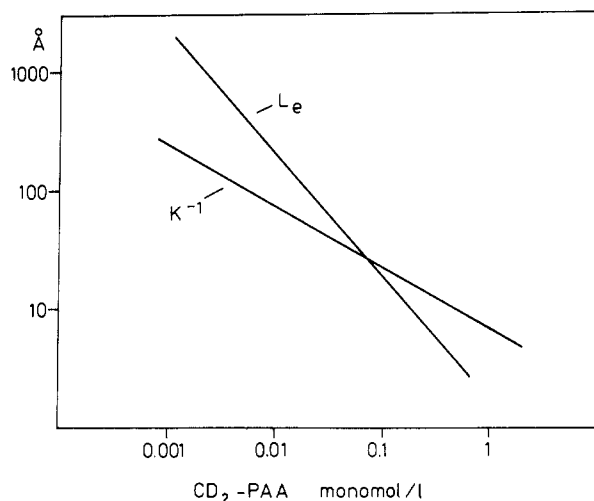


Figure 1. Concentration dependence of the electrostatic persistence length L_e and the Debye length κ^{-1} for a sodium polyacrylate solution. The intrinsic persistence length of PAA is in the order of 10 Å. Below 0.1 monomol/L one can expect an altered dynamic response of the chains due to the increased total persistence ($L_t = L_p + L_e$) of the PAA chain.

where f is the effective dissociation parameter, the fraction of the polymer charge that is not compensated by associated or condensed counterions; κ^{-1} is the Debye screening length due to the small ions, $\kappa^2 = 8\pi Q c_s$ in excess salt conditions with c_s the concentration of added 1-1 electrolyte; Q is the Bjerrum length ($\equiv e^2/DkT$), the distance between two elementary charges chosen so that their electrostatic energy equals kT ($Q = 7.14$ Å in water at 298 K); A is the effective intercharge distance on the polyion; A can be viewed as the effective monomer length in case each monomer bears one elementary charge ($A = 2.5$ Å for a fully charged polyacrylate chain); λ is the charge density parameter, $[\equiv e^2/DkT = Q/A]$.

A characteristic distance is the Bjerrum length Q . As long as the intercharge distance A exceeds the Bjerrum length the effective dissociation parameter is 1 ($\lambda < 1$). In case the Bjerrum length Q exceeds the intercharge distance A an enhanced screening is predicted ($f = 1/\lambda = A/Q$).

In the salt-free case of highly charged polyelectrolytes ($f = A/Q$) one can redefine⁴ the Debye screening length as $\kappa^2 = 4\pi A C_p$ with C_p the equivalent monomer concentration, or in the case of slightly charged polyelectrolytes ($f = 1$) by $\kappa^2 = 4\pi Q C_p$. The addition of salt (NaCl) contributes to κ^2 another term $8\pi Q c_s$ with c_s the concentration of added salt.

The relation between κ^{-1} and L_e as a function of the concentration of a salt free fully neutralized CD_2 PAA solution is depicted in Figure 1. Below 0.1 monomol/L the electrostatic persistence length L_e exceeds the Debye length κ^{-1} whereas between 0.1 and 1 monomol/L κ^{-1} exceeds L_e . However, κ^{-1} exceeds L_e by not more than 10 Å, so the approximation of local stiffness $L_t = L_p + L_e > \kappa^{-1}$ is valid if $L_p > 10$ Å. In fact, the bare persistence length of PAA is about 10 Å, so the approximation of local stiffness seems to be justified for PAA at all concentrations.

For a concentration less than 0.1 monomol/L, L_t becomes significantly greater than L_p . Below this concentration one can expect an altered dynamic response of the chain due to the in-

(3) Muroga, Y.; Noda, I.; Nagasawa, M. *Macromolecules* **1985**, *18*, 1576.

(4) Katchalsky, A. *Pure Appl. Chem.* **1971**, *26*, 327.

(5) Odijk, T. *J. Polym. Sci., Polym. Phys. Ed.* **1977**, *15*, 477.

(6) Skolnick, J.; Fixman, M. *Macromolecules* **1977**, *10*, 944.

(7) Odijk, T.; Houwaart, A. C. *J. Polym. Sci., Polym. Phys. Ed.* **1978**, *16*, 627.

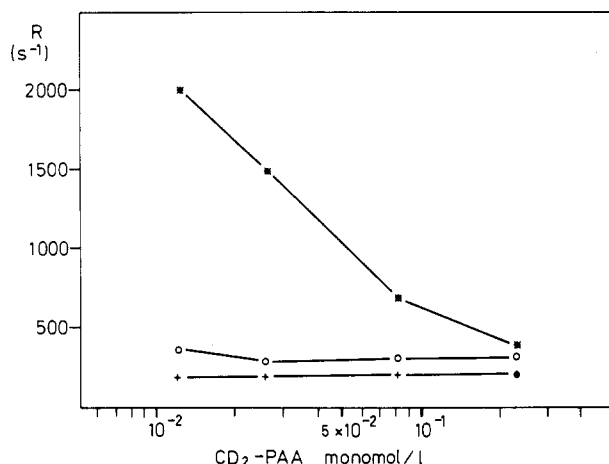


Figure 2. Concentration dependence of the relaxation rates ($\omega_0 = 41.4$ MHz, $\alpha = 0.78$ and DP = 850). The longitudinal relaxation rate R_1 (+) remains unchanged upon dilution, whereas the transversal relaxation rate is described by two exponentials (R_{2s} (O), R_{2t} (*)). R_{2s} is slightly greater than R_1 and remains nearly unchanged upon dilution. R_{2t} strongly increases upon dilution. Lines are drawn as an aid to the eye.

creased total persistence length.

Results

Nuclear magnetic relaxation rates of main-chain (methylene) deuterons of poly(acrylic acid) have been measured in the concentration range 0.01–0.2 mol/L, and for two distinct degrees of neutralization (0.1 and 0.78), see Table I, Figure 2. The degree of neutralization α is defined to be the ratio of added base (NaOH) and the number of carboxylic groups (when $\alpha = 1$, all acid groups are neutralized and the PAA chain is maximally charged). The results (Table I) show that R_1 and R_2 at $\alpha = 0.1$ as well as at $\alpha = 0.78$ are sensitive to the Larmor frequency ω_0 . This means that a dynamic process must be involved with a correlation time $\tau \approx 1/\omega_0 \approx 10^{-9}$ s.

As discussed below the transverse relaxation is not simple exponential and it may be represented by a biexponential decay. In this preliminary analysis the general behavior of the average transverse rate R_2 and the longitudinal rate R_1 will be discussed.

The effect of dilution and neutralization is very remarkable. The longitudinal relaxation rate R_1 essentially remains unchanged upon altering the concentration, whereas the transverse relaxation rate R_2 sharply increases in case the solutions are both diluted and neutralized.

Given this fact of a sharply increased R_2 in the semidilute regime and an essentially unchanged (but still frequency-dependent) R_1 one has to conclude that in this regime a new dynamical process appears with a correlation time $\tau \gg 1/\omega_0$.

The nuclear magnetic relaxation rates are closely related to reduced spectral density values $\tilde{J}(\omega)$.⁸

$$R_1 = (12\pi^2/80)(e^2qQ/h)^2(1 + \eta^2/3)[\tilde{J}(\omega_0) + 4\tilde{J}(2\omega_0)]$$

$$R_2 = (12\pi^2/160)(e^2qQ/h)^2(1 + \eta^2/3)[3\tilde{J}(0) + 5\tilde{J}(\omega_0) + 2\tilde{J}(2\omega_0)] \quad (3)$$

where ω_0 is the Larmor frequency and e^2qQ/h is the coupling constant of the quadrupole interaction with the CD bond and is chosen to be 170 ± 5 kHz.⁹ The asymmetry parameter η of the CD bond is neglected in our calculations. As it seems that for this new and presumably independent process the contribution to R_2 is much greater than the contribution to R_1 one may roughly estimate a correlation time: $R_2 \gg R_1 \rightarrow \tilde{J}(0) \gg \tilde{J}(\omega_0), \tilde{J}(2\omega_0)$; $R_2 \simeq (e^2qQ/h)^2 36\pi^2 \tilde{J}(0)/160$. If this process obeys a Lorentzian

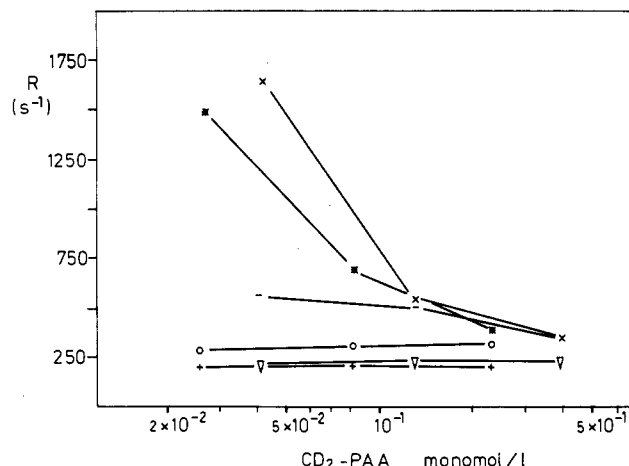


Figure 3. Dependence of the relaxation rates on polymer concentration for two different degrees of polymerization. For DP = 850, $\alpha = 0.78$; (*) R_{2t} , (O) R_{2s} , (+) R_1 . For DP = 5000, $\alpha = 0.8$; (X) R_{2t} , (-) R_{2s} , (∇) R_1 . The longitudinal relaxation rates are not sensitive to the degree of polymerization. The transverse relaxation rates are slightly larger for the samples with a higher degree of polymerization.

behavior, i.e., $\tilde{J}(\omega) = 2\tau/(1 + \omega^2\tau^2)$ then for $\tau \gg 1/\omega_0$ one has $\tilde{J}(0) \approx 2\tau$ and for $R_2 \approx 1000$ this yields $\tau \approx 1 \times 10^{-8}$ s.

With regard to the determination of the transverse relaxation rate R_2 an interesting observation is made in the region $R_2 \gg R_1$; it is no longer possible to characterize the transverse decay curve with a single exponent. The decay curve of its Fourier transform, the line-shape curve, may be represented with a double exponent or a double Lorentzian fit. However, due to the limited accuracy of the decay curve, it is not possible to conclude whether two, three, or more exponents are needed in characterizing the decay curve.

Representing the transverse decay by two exponentials of equal amplitude leads to good fit results. The effect of polymer charge density and polymer concentration appear amplified in the largest of the two transverse rate constants, R_{2t} (Table I, Figure 2).

In Figure 3 it is shown that the effect of the degree of polymerization (DP) is moderate in the concentration regime that was investigated. The effect of DP may be somewhat masked in the present results due to the fact that the polymer fractions used are not very narrow ($M_w/M_n > 2$).

From the considerations above it may be concluded that besides the deduced existence of at least two motional processes, there are at least two motionally distinctive kinds of CD bonds in the polyacrylic chain. This presents an interesting problem for the interpretation of the relaxation rates in terms of (motional) spectral density values and corresponding correlation times for the dynamic processes involved.

As discussed in the Introduction (Figure 1) the electrostatic persistence length is expected to show an important increase in the region below 0.1 monomol/L CD₂-PAA. In the same region a strong increase of the transverse relaxation rate is observed. The emergence of the large correlation times (Figure 2) may therefore be correlated with the increased total persistence of the polyelectrolyte chain due to the diminished shielding of the chain charges by the counterions. This interpretation may be verified by adding a little salt to the solution. Only the Debye screening length is modified by adding salt. In Figure 4 it is seen that R_{2t} is indeed extremely sensitive to the concentration of added salt. At roughly equivalent polyion and added salt concentrations the "dilution effect" on R_{2t} has nearly disappeared.

In the following section these observations will be pursued in a more quantitative, though approximate, manner. At this stage the nonexponential character of the transverse decay should be discussed. This behavior appears on dilution of the polymer solution (Table I). As indicated above, the decay curve may be fitted within experimental error with two equally weighted exponentials. This does not exclude the possibility that the decay is in fact multiexponential. Several explanations for the nonexponential decay may be proposed.

(8) Abragam, A. *The Principles of Nuclear Magnetism*; Clarendon: Oxford, UK, 1961.

(9) Grandjean, J.; Sillescu, H.; Willenberg, B. *Makromol. Chem.* **1977**, *178*, 1445.

TABLE II: Spectral Density Values^a of CD₂-PAA Corresponding to the Relaxation Rates of Table I

set no.	frequency, MHz					
	0	4.6	9.2	18.4	41.4	82.8
J _{s1}	204 ± 16	207 ± 14	190 ± 7	170 ± 7	141 ± 16	88 ± 8
J _{f1}	355 ± 20	199 ± 13	192 ± 6	170 ± 7	123 ± 15	92 ± 8
J _{s2}	244 ± 16	194 ± 13	194 ± 6	136 ± 7	121 ± 16	97 ± 8
J _{f2}	840 ± 50	232 ± 13	185 ± 6	138 ± 7	112 ± 16	99 ± 8
J _{s3}	204 ± 16	206 ± 13	194 ± 6	146 ± 7	111 ± 16	94 ± 8
J _{f3}	2080 ± 150	219 ± 14	191 ± 6	147 ± 6	113 ± 15	94 ± 8
J _{s4}	332 ± 20	209 ± 13	194 ± 6	126 ± 7	108 ± 16	84 ± 8
J _{f4}	2900 ± 200	246 ± 15	185 ± 6	129 ± 7	99 ± 15	87 ± 8

^aReduced spectral density in 10⁻¹¹ s. The values are obtained by linear transformation of the set (R₁, R_{2s}) and (R₁, R_{2f}) at three frequencies for each sample. Errors are directly determined by the linear transformation and range from 5 to 20%.

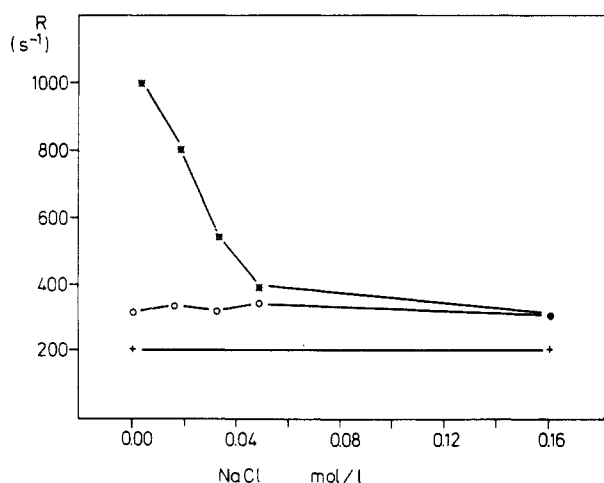


Figure 4. Dependence of the relaxation rates on the concentration of NaCl (CD₂PAA, 0.042 monomol/L, DP = 850, α = 0.78). Meaning of the symbols: (+) R₁, (O) R_{2s}, (*) R_{2f}. Lines are drawn as an aid to the eye. R_{2f} collapses to the value of R_{2s} at high added salt (NaCl) concentrations. Compare the concentration dependence of Figure 1 and also Figure 6.

Dependence on the Degree of Polymerization. In principle, polydispersity of the polymer samples might be responsible. However, if the macromolecules are sufficiently long,¹⁰ one can neglect end effects and the NMR measurements must become independent of the degree of polymerization. Even when the sample is polydisperse there will be no effect on the relaxation rates. In fact, measurements on samples of different DP (Figure 3) do reveal only slightly different relaxation rates, while the double exponential character remains, so the dispersion in the DP cannot solely explain the observed nonexponential decay. If the observed relaxation rates are due to some "average" monomer, reorienting according to a given diffusion tensor, the occurrence of two distinct deuterons in the monomer could explain the observation because different CD bonds will then have different orientations with respect to the diffusion tensor. This effect may be split in two parts.

Tacticity of the Polyacrylate Chain. The methylene-deuterated poly(acrylic acid) CD₂-PAA has been synthesized by using a radical mechanism usually leading to atactic polymers. High-resolution spectra of CD₂PAA have confirmed this notion. Quantitative analysis of these spectra reveals an equal amount of syndio- and isotactic configurations in CD₂-PAA. Depending on the succession of syndio and isotactic configurations, the CD₂-PAA chain will possess differently connected units. Consequently the CD bonds attached to each unit have a different mean orientation relative to the polyacrylate chain. If the average reorientational behavior of a monomer depends on the tacticity this offers an explanation for the (at least) double-exponential transverse relaxation.

Each Monomer Contains Two Deuterons. Apart from the complicating tacticity contribution each monomer possesses two

deuterons, so that even in the advantageous case of a pure isotactic or syndiotactic CD₂-PAA chain there are two differently oriented CD bonds per monomer present in the chain and this will lead in principle to a double-exponential behavior.

If one excludes polydispersity in explaining the nonexponential transverse decay curve one has to conclude that the motional processes within one chain must be separated into at least two motional groups of deuterons. The following representation of the local polymer motion may then be advanced as a suitable context for the interpretation of our NMR results. Most of the quadrupole coupling of the polymer deuterons is averaged by fast local reorientations. Only a small part of the quadrupole coupling left is averaged by sufficiently slow motions of parts of the polymer chain to cause a dispersion in the relaxation rates. A distribution of relaxation rates due to a distribution of effective CD orientations with respect to the principle diffusion axis that represents the fast motions may show up in the transverse relaxation because it is sensitive to slow motion. Due to the limited experimental accuracy, (measurements are performed in the dilute regime) a full characterization of this distribution is impossible at present. The transverse decay is clearly nonexponential, but two exponentials suffice to reproduce it and a larger number of exponents cannot be significantly characterized. The two transverse relaxation rates that can be extracted from the decay should, in this context, reflect the width of the distribution of the rates. This distribution is due to the effective distribution of the orientation of the CD bonds during fast motions that average out most of the quadrupole coupling. Since the transverse relaxation curve is well described by a double-exponential decay, the experimental results will be transformed into two sets of spectral densities. These are calculated from the two transverse rates, each of which is combined with the observed single longitudinal rate to form the sets (R₁, R_{2f}) and (R₁, R_{2s}). Provided that the ratio of two of the three experimental Larmor frequencies equals two (in the present case 4.6, 9.2, and 41.4 MHz) it is possible to compute the spectral density values by linearly transforming each set of six relaxation rate equations with an equal number of unknowns (Table II).

In the next section the spectral density function for quadrupolar coupling as modulated by polymer motion will be presented, mainly in the context of the representation of local polymer motion discussed above. In the subsequent section the theoretical parameters will be determined by fitting the theoretical spectral density function to the experimental results. These parameters will then be discussed in terms of a crude hydrodynamical representation of the polymer motion on a large timescale (>10⁻⁹ s).

Spectral Density and Polymer Motion

Macromolecules exhibit many types of motion of widely different rates and character. However, it is possible to introduce a number of simplifying assumptions by which one divides the possible modes into a number of types, any one type having a particular advantage in describing the motion.

One discerns, for instance, motions, involving large segments of the chain as anisotropic reorientation^{11,12} and overall tumbling,

(10) Heatly, F. *Prog. NMR Spectrosc.* **1979**, *13*, 47.

(11) Woessner, D. J. *Chem. Phys.* **1962**, *36*, 1.

or local motions involving the internal rotation of only a few monomers initiated by the conformational transitions and the Brownian force of the surrounding solvent.

Relating the obtained spectral densities to reasonably well-defined modes of polymer motion in the solution is thus a difficult and tentative process. For poly(methacrylic acid) it was found¹³⁻¹⁵ that three correlation times were necessary to represent the spectral density for the methylene deuteron relaxation. In a simple rotation diffusion model for the "average" monomeric unit these three correlation times may be derived from either two or three diffusion tensor elements. It has been pointed^{16,17} out that the three-exponential correlation function from which the three correlation times are derived may represent at least three different motional models. These models are

(a) axially symmetric overall rotation diffusion (D_{\perp}, D_{\parallel}) with correlation times

$$\tau_0 = (6D_{\perp})^{-1}, \quad \tau_1 = (5D_{\perp} + D_{\parallel})^{-1}, \quad \tau_2 = (2D_{\perp} + 4D_{\parallel})^{-1}$$

(b) axially symmetric overall rotation diffusion combined with an internal rotation diffusion (D_i) about an axis parallel with D_{\parallel}

$$\tau_0 = (6D_{\perp})^{-1}, \quad \tau_1 = (5D_{\perp} + D_{\parallel} + D_i)^{-1}, \quad \tau_2 = (2D_{\perp} + 4D_{\parallel} + 4D_i)^{-1}$$

(c) spherical overall rotation diffusion (D_0) combined with an internal rotation diffusion D_i

$$\tau_0 = (6D_0)^{-1}, \quad \tau_1 = (6D_0 + D_i)^{-1}, \quad \tau_2 = (6D_0 + 4D_i)^{-1}$$

Therefore, even within the context of the simple rotation diffusion description the relation of the correlation times and a concrete motional model is not unique. In fact, the choice for a model may depend on the chemical nature of the polymer involved. For a rather stiff polymer such as poly(methacrylic acid), model a seems reasonable, whereas for a highly flexible polymer model c may be appropriate.

Irrespective of the specific rotation diffusion model involved, the spectral density $\tilde{J}(\omega)$ in eq 2 is related to the time correlation function of the irreducible components $B_m^{(2)}$ of the electric field gradient tensor at the ^2H nucleus involved according to

$$\begin{aligned} \tilde{J}(\omega) &= \frac{1}{G_m^{(0)}} \int_{-\infty}^{\infty} G_m(\tau) e^{-i\omega\tau} d\tau = \\ &= \frac{1}{G_m^{(0)}} \int \langle B_m^{(2)}(0) B_m^{(2)*}(\tau) \rangle_{\text{LAB}} e^{-i\omega\tau} d\tau \\ &= \frac{1}{5G(0)} \int_{-\infty}^{\infty} \sum_k \langle \bar{B}_k^{(2)}(0) \bar{B}_k^{(2)*}(\tau) \rangle_{\text{DIF}} e^{-\tau/\tau_k} e^{-i\omega\tau} d\tau \quad (4) \\ &= \frac{2}{3(1 + \eta^2/3)(eq)^2} \int_{-\infty}^{\infty} \sum_k \langle \bar{B}_k^{(2)}(0) \bar{B}_k^{(2)*}(\tau) \rangle_{\text{DIF}} e^{-\tau/\tau_k} e^{-i\omega\tau} d\tau \end{aligned}$$

Here, B and \bar{B} are defined in the laboratory coordinate system (LAB) and the principal axis system of the diffusion tensor (DIF), respectively. DIF refers to either the overall tensor in model a and b or the internal rotation axis in model c.

In the present models the $\bar{B}_k^{(2)}$ contain no further time dependence. They may be related to the field gradient components on a molecular reference system (REF), which is defined with the x axis along the bisectrix of the CD_2 internal angle and with the z axis connecting the D nuclei

$$\bar{B}_k^{(2)} = \sum_m \bar{B}_m^{(2)} D_{mk}^{(2)}(\alpha, \beta, 0) = \sum_m F_0^{(2)} D_{0m}^{(2)}(0, \beta^{\pm}, 0) D_{mk}^{(2)}(\alpha, \beta, 0) \quad (5)$$

The last equality relates $\bar{B}_m^{(2)}$ to the single tensor component $F_0^{(2)} = (2/3)^{-1/2} eq$ in the electric field gradient principal axis system

at a deuteron if the asymmetry parameter η is neglected. The angles β^{\pm} are defined by the z axis of REF and the two CD bonds, i.e. $\beta^{\pm} = 35.25^\circ$ or 144.75° . The angles α and β relate the DIF and REF systems. Thus, one has for $\tilde{J}(\omega)$

$$\tilde{J}(\omega) = \sum_k |\sum_m D_{0m}^{(2)}(0, \beta^{\pm}, 0) D_{mk}^{(2)}(\alpha, \beta, 0)|^2 \frac{2\tau_{|k|}}{1 + \omega^2 \tau_{|k|}^2} \quad (6)$$

The $\tau_{|k|}$ depend on the motional model as specified before. If a distribution of the CD-bond orientations with respect to the diffusion tensor principal axis is expected, the introduction of the intermediate reference frame REF serves no useful purpose. Instead \bar{B}_m in the DIF system may directly be related to $F_0^{(2)}$ in the field gradient system, again neglecting the asymmetry parameter η . Then for a single CD orientation

$$\tilde{J}(\omega; \beta) = \sum_k |D_{0k}^{(2)}(0, \beta, 0)|^2 \frac{2\tau_{|k|}}{1 + \omega^2 \tau_{|k|}^2} \quad (7)$$

The distribution of the CD orientations β then leads to a distribution of relaxation rates; i.e., the observed decay is a sum of exponentials. Provided that the spread in the distribution is small, the distribution is well characterized by two angles $\beta \pm \Delta\beta$ (a mean angle β and a spread $\Delta\beta$).

Relation 7 may then be transformed to

$$\tilde{J}_{f.s.}(\omega) = \sum_k |D_{0k}^{(2)}(0, \beta \pm \Delta\beta, 0)|^2 \frac{2\tau_{|k|}}{1 + \omega^2 \tau_{|k|}^2} \quad (8)$$

$D_{ij}^{(2)}$ is the Wigner rotation elements of second-rank tensor; $\beta \pm \Delta\beta$ is the Euler angles between the CD bonds and the diffusion tensor; $\tau_{|k|} = [D_{\perp} + k^2(D_{\parallel} - D_{\perp})]^{-1}$ and D_{\perp} and D_{\parallel} are the diffusion rates of a rotation ellipsoid.

Relation between Molecular Conformation and Diffusion Parameters

The relation between conformational and dynamical properties of macromolecules is a very delicate one. To obtain some insight it may be worthwhile to relate the rotation diffusion parameters to the theoretical dimensions of an ellipsoid of revolution for which Perrin¹⁸ derived the appropriate expressions.

For reference purpose expressions will be presented here relating diffusion tensor elements of model a (axially symmetric overall rotation) and model c (spherical overall rotation and one internal rotation) to the dimensions of the relevant motional units. Model a will be represented with a Perrin¹⁸ prolate ellipsoid of revolution with the rotation diffusion constants

$$D_{\perp}^{-1} = 32\pi\eta L_{\perp}^3 [p^2(1 - p^2)/(2 - p^2S)]/3kT \quad (9)$$

$$D_{\parallel}^{-1} = 32\pi\eta L_{\perp}^3 [(1 - p^4)/(S(2 - p^2) - 2)]/3kT$$

where $S = 2 \ln [(1 + (1 - p^2)^{1/2})/p]/(1 - p^2)^{1/2}$; L_{\perp} is the length of the long semiaxis; L_{\parallel} is the length of the short semiaxis; p is the ratio L_{\perp}/L_{\parallel} ; and η is the viscosity of the fluid medium. The long semiaxis (L_{\perp}) can be considered a measure of the dynamic stiffness of the polymer chain.

In model c the overall rotation of a sphere with a hydrodynamical radius L_0 is used with the rotation diffusion constant D_0 .

$$D_0^{-1} = 8\pi\eta L_0^3/kT \quad (10)$$

Model b results in a prolate ellipsoid with dimensions in between those of model a and the sphere c and will not be treated here.

Analysis of the Experimental Data

The two sets of spectral densities calculated from the relaxation rates (R_1, R_2) and (R_1, R_{2s}) were used to determine the correlation times in eq 8 using a least-squares fit procedure. A representative result is shown in Figure 5. The result of this procedure is a set of three correlation times (i.e., two diffusion constants) and the two orientations $\beta \pm \Delta\beta$, one for each of the sets (R_1, R_{2f}) and

(12) Wallach, D. J. *Chem. Phys.* **1967**, *47*, 5258.

(13) Schriever, J.; Joosting Bunk, J.; Leyte, J. C. *J. Magn. Reson.* **1977**, *27*, 45.

(14) Mulder, C. W. R.; Schriever, J.; Leyte, J. C. *J. Phys. Chem.* **1985**, *89*, 475.

(15) Mulder, C. W. R.; Leyte, J. C. *J. Phys. Chem.* **1985**, *89*, 1007.

(16) Schriever, J. et al. *Ber. Bunsenges. Phys. Chem.* **1977**, *81*, 287.

(17) Huntress Jr., W. T. *Adv. Magn. Reson.* **1970**, *4*, 1.

(18) Perrin, F. *J. Phys. Radium* **1934**, *5*, 497.

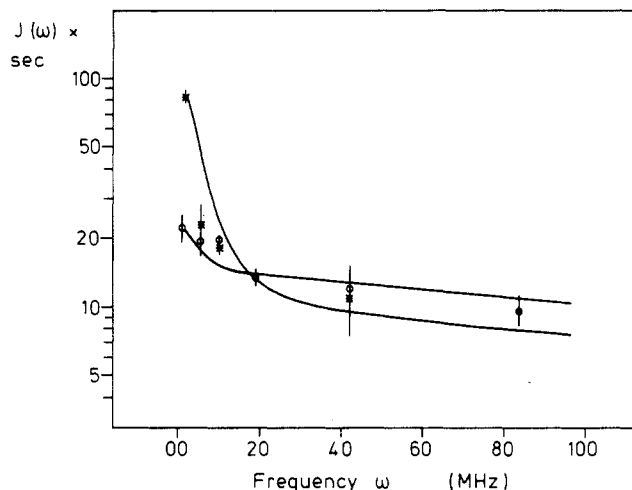


Figure 5. Reduced spectral density $J_{\parallel}(\omega)$ (*) and $J_{\perp}(\omega)$ (O) corresponding respectively to the sets (R_1, R_{2f}) and (R_1, R_{2s}) of sample 3 (0.026 monomol/L CD₂PAA, $\alpha = 0.78$). Drawn lines result from a simultaneous fit of the points to the rotation diffusion model eq 8.

TABLE III: Fit Results of the Rotation Diffusion Model^a

no.	C_p	α	$D_{\perp}^{-1} \pm \Delta D_{\perp}^{-1}$, ns	$D_{\parallel}^{-1} \pm \Delta D_{\parallel}^{-1}$, ns	β , rad	$\Delta\beta$, rad
S ₁	0.23	0.78	71 ± 10	0.74 ± 0.04	0.8	0.007
S ₂	0.082	0.78	232 ± 16	0.73 ± 0.03	0.8	0.042
S ₀	0.026	0.78	447 ± 26	0.89 ± 0.04	0.8	0.09
S ₄	0.012	0.78	651 ± 34	0.84 ± 0.03	0.8	0.085

^a The spectral density function of a reorienting ellipsoid was fitted using a weighted least-squares algorithm to the spectral density values of Table II. The algorithm fits simultaneously the rotation diffusion model with two angles to the spectral density values $J_{\parallel}(\omega)$ and $J_{\perp}(\omega)$ for each sample.

TABLE IV: Transformation of the Rotation Diffusion Constants D_{\perp} and D_{\parallel} to Model a, the Long and Short Semiaxes of a Perrin Ellipsoid, and Model c, the Radius of a Reorienting Sphere (Using only D_0)^a

no.	D_{\perp}^{-1} , ns	D_{\parallel}^{-1} , ns	L_{\perp} , Å	L_{\parallel} , Å	L_0 , Å	L_t , Å
S ₁	71	0.74	52	2.0	25	16
S ₂	232	0.73	82	1.6	37	28
S ₃	447	0.89	104	1.6	46	66
S ₄	651	0.84	120	1.4	51	131

^a For the viscosity of the surrounding fluid the value of pure water at 25 °C is used.

(R_1, R_{2s}) . At the value of β found in this way, the relatively small value of $\Delta\beta$ exerts its main effect at low frequencies; at high frequencies the two spectral densities lead to experimentally inseparable longitudinal decays. In Table III diffusion constants are shown as calculated from the correlation times according to model a, axially symmetric rotation diffusion. It is seen that the slow motions that emerge on diluting the polymer are reflected in D_{\perp} . This parameter increases from 70 to 650 ns upon dilution, i.e., upon reducing the ionic strength, thereby increasing the electrostatic persistence length. Using the relations for the τ_k the data of Table III may be easily transformed to obtain D_0 and D_1 of model c, spherical overall rotation diffusion. In Table IV the motional parameters (D_{\perp} , D_{\parallel} , and D_0) were transformed into dynamic persistence lengths (L_{\perp} , L_{\parallel} , and L_0) according to (9) and (10). The spherical model approach shows an increase of the radius of the representative sphere from 25 to 51 Å upon dilution from $C_p = 0.23$ to 0.012 monomol/L CD₂-PAA. At the same polymer concentrations the ellipsoidal model shows an increase of the long semiaxis from 52 to 120 Å.

From the electrostatic persistence length L_e (Table IV) it is seen that, with an estimated intrinsic persistence length $L_p \approx 10$ Å, the total persistence length $L_t = L_p + L_e$ increases from roughly 16 to 130 Å. It seems therefore that at the high concentrations where the polymer is still rather flexible due to a short screening

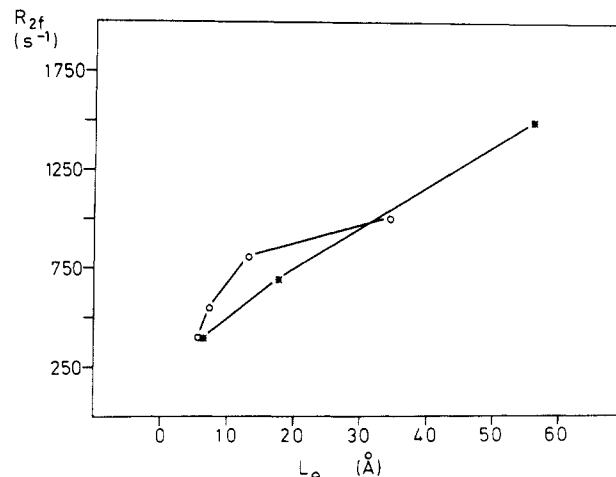


Figure 6. Correlation between the electrostatic persistence length and the fast transverse relaxation R_{2f} . The results of the concentration dependence of Table I (*, R_{2f}) and the added salt concentration of Figure 4 (O, R_{2f}) are scaled to the persistence length L_e and depicted in one figure. Values chosen for the interchange distance $A = 2.5/\alpha$ Å ($\alpha = 0.78$) and for the Bjerrum length $Q = 7.14$ Å.

length, the spherical model is appropriate in representing the correlated reorientational motion of a number of monomeric units. On dilution the screening length increases and the polymer coils will stretch. In this region the ellipsoidal model appears to be in reasonable agreement with the theoretical values for L_t . Apart from the approximate nature of the used models a and c, the agreement with predictions from polyelectrolyte theory seems encouraging.

In describing the motion of a polyelectrolyte chain we tacitly assumed that the effective viscosity η will not change upon dilution. Fortunately, the dimensions of neither the Perrin ellipsoid nor the reorienting sphere are very sensitive for the precise value of the viscosity ($L_{\perp} \propto \eta^{-1/2}$ and $L_0 \propto \eta^{-1/3}$).

In case a simple salt (NaCl) is added to the solution (increasing the ionic strength) the fast transverse relaxation rate contracts to the slow transversal rate (Figure 4) and the slow motions disappear.

We suppose that the increase of the transverse relaxation rate originates from the increasing of the electrostatic persistence length. This idea may be verified in the following manner. The electrostatic persistence length is determined by the Debye length (eq 2). The Debye length in its turn is determined by the counterion and added salt concentration via the relation⁴ $\kappa^2 = 8\pi Q(c_s + AC_p/2Q)$. The separate behavior of the dilution of the polymer solution and the addition of salt at a fixed polymer concentration may be represented in one figure by using this relation with the Debye length (or the electrostatic persistence length using relation 2) as the only free parameter.

In Figure 6 the relation between the (fast) relaxation rate and the electrostatic persistence length is depicted. Use has been made of the following values: $A = 2.5/\alpha$ Å ($\alpha = 0.78$) and $Q = 7.14$ Å. Apparently there is a direct correlation between the electrostatic persistence length and the fast transverse relaxation rate. The results suggest that the behavior of the transverse relaxation rate on diluting the polymer and on changing the simple salt concentration is in both cases dependent of changes of the electrostatic persistence length.

Relation between Polyion and Counterion Relaxation

The present results on the relaxation of polymer-deuteron nuclei have an important conceptual implication for the interpretation of the quadrupolar relaxation of counterions in polyelectrolyte solutions. The transverse relaxation R_{2f} of ²³Na in polyelectrolyte solutions shows an important increase on diluting a polyelectrolyte salt below a concentration of roughly 0.1 monomolar.¹⁹ Analysis

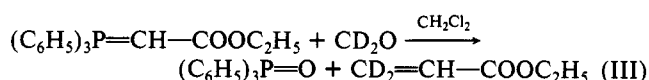
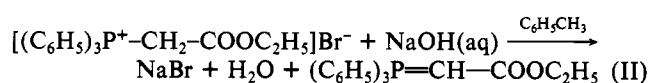
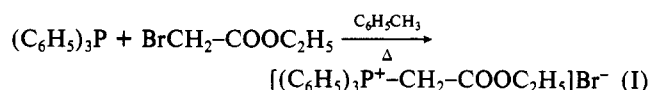
(19) Levy, M.; De Bleijser, J.; Leyte, J. C. *Bull. Magn. Reson.* **1980**, *2*, 388.

of the results¹⁹ shows that the appearance of a long correlation time upon diluting the solution is responsible for the increase of the fast transverse relaxation rate. This phenomenon is extremely sensitive to the addition of a mono-monovalent salt.

Several explanations^{20,21} have been put forward to describe the effect. In the explanation of Halle et al.²¹ the basic argument states that counterions have to leave a given polyion domain and diffuse to another polyion in order to be able to reduce the correlation function of the electric field gradient to zero. On enlarging the interpolymer distance by dilution, this process introduces large correlation times. The present results on polymer-deuteron relaxation demonstrate that a quadrupolar nucleus bound to the polymer shows qualitatively the same behavior as the mobile sodium counterions. Therefore, interpolymer diffusion is not a necessary cause to explain the effect. A strong dynamic correlation (not necessarily binding) of the counterion and the polyion should be sufficient to explain the relaxation behavior of the counterions in semidilute polyelectrolyte solutions.

Experimental Section

Synthesis of Acrylic Acid- β - d_2 . The ethyl ester of acrylic acid- β - d_2 was synthesized by a Wittig²² reaction according to the following reaction scheme:



Ethoxycarbonylmethylenetriphenylphosphonium Bromide²³ (1). Triphenylphosphine (180 g) is dissolved in 1200 cm³ of toluene. To this solution is added, with stirring, a solution of 116 g of ethyl bromoacetate in 300 cm³ of toluene. The mixture is heated to 60 °C and maintained at this temperature for 10 min. After cooling the mixture is kept at room temperature overnight. The crystals are filtered, washed with pentane, and dried.

Ethoxycarbonylmethylenetriphenylphosphorane²⁴ (2). Eighty-six grams of **1** is dispersed in 2 L of toluene and 2 L of 0.38 N NaOH solution. The mixture is stirred vigorously for 1 h. The toluene layer is separated off and dried with anhydrous sodium sulfate. It is then evaporated under reduced pressure to yield the crude product **2**. **2** is purified by recrystallization from ethyl acetate/petroleum spirit 60/80.

Ethyl Acrylate- β - d_2 ²⁵ (3). The apparatus consisted of a two-necked 1-L round-bottomed flask supplied with a magnetic stirrer, an inlet tube for deuterioformaldehyde and a short Claisen condenser carrying a bubble flask with paraffin oil. In the flask was introduced a solution of 253 g of **2** in 800 cm³ of CH₂Cl₂. In the inlet tube a plug of glass wool was inserted and 24.8 g of perdeuterioparaformaldehyde (D min 99%) was brought in. Nitrogen gas was led over the deuterioparaformaldehyde and the reaction flask cooled in ice.

The deuterioparaformaldehyde was depolymerized slowly by carefully heating the inlet tube with a flame. The formaldehyde gas formed was carried with the nitrogen into the solution of **2**. After the deuterioformaldehyde was introduced stirring was continued for 1 h.

After 650 mL of CH₂Cl₂ was distilled out from a Widmer column. The residual volatile products were collected in a liquid nitrogen trap under moderately reduced pressure and then fractionally distilled under nitrogen.

The yield of pure product (checked by GLC) was ~80%. The NMR spectrum of the ethyl acrylate- β - d_2 showed no absorptions for undeuteriated methylene protons. After saponification of the ethyl ester, acrylic acid- β - d_2 was obtained and subsequently polymerized under nitrogen in an aqueous solution with H₂O₂²⁶ as initiator at a temperature of 85 °C for a period of 4 h. The polymer solution was cooled down, freeze dried, and fractionated, followed by dialysis and freeze drying. Four fractions were obtained with corresponding molecular weights 61.000, 153.000, 183.000, and 356.000 as determined by viscosity measurements using the Houwink-Sakurada equation $[\eta] = KM^\alpha$. For PAA in 0.01 N HCl, $K = 0.68 \times 10^{-3}$ and $\alpha = 0.5$ at 300 K.

Sample Preparation

The methylene-deuteriated poly(acrylic acid) (CD₂-PAA) was synthesized in this laboratory (see Synthesis of Acrylic Acid- β - d_2). The estimated deuterium purity was at least 98% based on the quantitative study of high-resolution NMR spectra of the CD₂-PAA sample. The obtained polydisperse product was fractionated first by successive precipitation from a methanolic polyacrylic solution with diethyl ether and subsequently by hyperfiltration using Spectrapor filters with specified MW cutoffs 3.500, 12–14.000, 50.000.

The samples were prepared by dissolving CD₂-PAA in deuterium-depleted water (Aldrich 19, 529-4; deuterium content 0.0033 \times Nat.Ab.) and neutralized with pro analyze NaOH (Merck 6498).

The NMR tubes consisted of quartz (diameter 10 mm) and were home made. The tubes were cleaned with sodium bicarbonate and EDTA.

NMR Measurements

The relaxation rates were determined at 4.6, 9.2, and 41.4 MHz. The measurements at the two lowest Larmor frequencies were performed on a home-built pulsed spectrometer equipped with a 2.1-T (max) Bruker electromagnet. The magnet is stabilized by a home-built field frequency lock using an external LiCl sample (saturated solution in DMF). The timing of the experiments was generated by a timing simulator (RS-648E, Interface Technology). Spectrometer control and data acquisition were performed by a LSI 11-23 microcomputer. The temperature of the sample was adjusted to 298 \pm 0.1 K by a fluid thermostat using Fluorinert FC-43 (3M). The measurements at 41.4 MHz were performed on a modified Bruker SXP spectrometer equipped with an Oxford Instrument 6.3-T superconducting magnet. The pulse program timing, spectrometer control, and data acquisition are identical with those of the low-field spectrometer. The samples were thermostated at 298 \pm 0.5 K by using a Bruker B-VT 1000 gas thermostat. Quadrature detection is used on both instruments.

Longitudinal relaxation times T_1 were determined with standard inversion recovery measurements, and transverse relaxation times T_2 were determined with free induction decays and/or spin-echo experiments.

Transverse relaxation data as determined by spin-echo experiments were fitted to single or double exponentials using the Marquardt-Levenberg algorithm.^{27,28}

Transverse relaxation data as determined by free induction decays were treated differently; these measurements were performed off resonance at half the Nyquist frequency, accumulated, and subsequently Fourier-transformed. In this way it was possible to separate the slowly varying base-line artifacts from the fast beating deuterium signal, a great advantage in case of low concentrations and low signal. Finally the deuterium Fourier spectrum

(20) Levy, M.; de Bleijser, J.; Leyte, J. C. *Chem. Phys. Lett.* **1981**, *87*, 183.

(21) Halle, B.; Wennerström, H.; Piculell, L. *J. Phys. Chem.* **1984**, *88*, 2482.

(22) Johnson, A. W. *Ylid Chemistry*; Academic: London, 1966.

(23) Armstead, D. E. F. *Education in Chemistry*; The Chemical Society: London, 1979; p 93.

(24) Denney, D. B.; Ross, S. T. *J. Org. Chem.* **1962**, *27*, 998.

(25) Isler, O.; Gutmann, H.; Montavon e.o., M. *Helv. Chim. Acta* **1957**, *40*, 1242.

(26) Alexandrowicz, Z. *J. Pol. Sci.* **1959**, *40*, 919

(27) Nash, J. C. *Compact Numerical Methods for Computers*; Adam Hilger: Bristol, U.K.

(28) Clifford, A. A. *Multivariate Error Analysis*; Applied Science: London, 1973.

was fitted to a single or a double Lorentzian and corrected for the shimmed line-width values of the magnetic field (of the order hertz). To be certain in exciting and observing all deuterons the signal amplitude of the free induction decay was checked with the expected value for each sample.

Conclusion

The increasing rate of the transverse relaxation of the deuterons in sodium polyacrylate is correlated with the increasing persistence length on diluting the solution. This is confirmed through varying the ionic strength at a fixed polymer concentration by adding NaCl to the solution.

A simple rotation diffusion model was presented to describe the experimental data. Two interpretations of this model were given to obtain a relation between the dynamic parameters (correlation times and dynamic persistence lengths) and the static

parameters (intrinsic and electrostatic persistence length).

It is found as a first approximation that at high concentrations a reorienting sphere with internal rotation adequately connects the relaxation rates with the persistence length. At low concentrations the persistence length is better approximated by a prolate ellipsoid model.

At present it seems that this model is very well capable of reproducing the double-exponential relaxation rates. Other models²⁹⁻³¹ on polymer motion (main chain dynamics) will be treated in a forthcoming paper.

Registry No. CD₂PAA·xNa, 104876-23-5.

(29) Valeur, J. P.; Geny, F.; Monnerie, L. *J. Polym. Sci., Polym. Phys. Ed.* **1975**, *13*, 667.

(30) Bendler, J. T.; Yaris, R. *Macromolecules* **1978**, *11*, 650.

(31) Skolnick, J.; Yaris, R. *Macromolecules* **1982**, *15*, 1041.

Measurement of Binary and Ternary Mutual Diffusion Coefficients of Aqueous Sodium and Potassium Bicarbonate Solutions at 25 °C

John G. Albright,* Roy Mathew,

Department of Chemistry, Texas Christian University, Fort Worth, Texas 76129

and Donald G. Miller

University of California, Lawrence Livermore National Laboratory, Livermore, California 94550

(Received: April 17, 1986; In Final Form: August 22, 1986)

Binary mutual diffusion coefficients are reported for NaHCO₃-H₂O and KHCO₃-H₂O at 25 °C for concentration ranges of 0.015–0.9 M. Experimental results are compared with those diffusion coefficients calculated from the Onsager-Fuoss theory. Thermodynamic diffusion coefficients are calculated. Ternary diffusion coefficients for NaHCO₃ (0.25 M)-KHCO₃ (0.25 M)-H₂O at 25 °C are reported. The results suggest that, up to 0.5 ionic strength for this system, ternary diffusion coefficients may be estimated within 1–2% accuracy from the experimental binary diffusion coefficients and the limiting ternary diffusion coefficients which are calculated from limiting ionic conductances. A few important partial molar properties of the ternary system are calculated by using Young's rule. Density measurements are reported for the KHCO₃-H₂O system up to 1.0 M.

Introduction

Sodium bicarbonate and potassium bicarbonate are important solutes in many aqueous systems found in nature, yet good experimental diffusion data for these systems have not been available. In 1941 Vinograd and McBain¹ reported data for the sodium bicarbonate system obtained by the diaphragm cell method. However, at that time, techniques for the method had not been refined, and the results obtained were subject to considerable error. Recently good quality data for the sodium bicarbonate system were reported by Leaist and Noulty² which had been obtained by the restricted-diffusion conductometric method.³ However, their data are for low concentrations and only extend up to about 0.1 M. Thus, there is still a need for good data at higher concentrations.

Experimental work reported here gives diffusion coefficients at 25 °C for sodium and potassium bicarbonate salts in aqueous binary solutions up to almost 0.9 M. The approximate saturation concentrations for NaHCO₃ and KHCO₃ at 25 °C are 1.18 and 3.15 M, respectively.⁴ The diffusion coefficients were measured by the free-diffusion method with either Rayleigh or Gouy types of interferometers.^{5,6} Thermodynamic diffusion coefficients were

calculated by using activity coefficients tabulated by Peiper and Pitzer⁷ and by Roy et al.⁸ Also presented here is one set of ternary diffusion coefficients measured at 25 °C at a mean concentration of 0.25 M for both solutes in water. The results suggest that ternary diffusion coefficients may be estimated from binary diffusion coefficients at concentrations up to 0.5 ionic strength for the system NaHCO₃-KHCO₃-H₂O.

Density measurements were made by pycnometry up to 1.15 M concentrations for aqueous solutions of potassium bicarbonate at 25 °C. At the time, the data of Larson et al.⁹ were unavailable.

Experimental Section

Chemicals. Mallinckrodt reagent grade NaHCO₃ and KHCO₃ were used without further purification for all experiments. Distilled water was used for preparation of all solutions. Values of 84.01 and 100.12 were used as the respective molecular weights of NaHCO₃ and KHCO₃.

Preparation of Solutions. At both TCU and Lawrence Livermore National Laboratory (LLNL), all solutions were prepared

(5) Gosting, L. J. *Advances in Protein Chemistry*, Academic: New York, 1956; Vol. 2, pp 429–554.

(6) Tyrrell, H. J. V.; Harris, K. R. *Diffusion in Liquids*, Butterworths: London, 1984.

(7) Peiper, J. G.; Pitzer, K. S. *J. Chem. Thermodyn.* **1982**, *14*, 613.

(8) Roy, R. N.; Gibbons, J. J.; Wood, M. D.; Williams, R. W.; Peiper, J. C.; Pitzer, K. S. *J. Chem. Thermodyn.* **1983**, *15*, 2017.

(9) Larson, J. W.; Zeeb, K. A.; Hepler, L. G. *Can. J. Chem.* **1982**, *60*, 2141.

(1) Vinograd, J. R.; McBain, J. W. *J. Am. Chem. Soc.* **1941**, *63*, 2008.

(2) Leaist, D. G.; Noulty, R. A. *Can. J. Chem.* **1985**, *63*, 2319.

(3) Harned, H. S.; French, D. M. *Ann. N.Y. Acad. Sci.* **1945**, *46*, 267.

(4) Linke, W. F. *Solubilities of Inorganic and Metal Organic Compounds*, 4th ed.; American Chemical Society: Washington, DC, 1956; Vol. 2.